Wind Speeds in Lower Atmosphere of Venus: Status Report on

Possible Measurement Via Differential VLBI

Tracking of Entry Probes

Irwin I. Shapiro

Department of Earth and Planetary Sciences

Massachusetts Institute of Technology

Cambridge, Massachusetts 02139

Abstract

The potential of very-long-baseline interferometry (VLBI)
is examined for use in the determination of wind speeds in
Venus' lower atmosphere via the differential tracking of entry
probes. A simplified mathematical model is presented in
detail. An incomplete error analysis based on this model
permits an educated guess to be made: An uncertainty in wind
speed determination of no more than about $100t^{-1}$ m/sec, where
t>1 is the corresponding time resolution in seconds, is an
achievable goal -- without the use of transponders on the
miniprobes. Certain important issues raised in the report
must be resolved before firm conclusions can be drawn. However,
if transponders are available on all probes, there should be
little difficulty in estimating wind speeds with useful
precision.

(Prepared for the Pioneer-Venus Science Steering Group)

May, 1972

_i._

Table of Contents

I. Introduction

Can the Venus entry probes be tracked via differential very-long-baseline interferometry (VLBI) with sufficient accuracy to yield useful estimates of the wind speeds in Venus' lower atmosphere? A definitive answer cannot yet be given. The current status of the analysis is summarized in this report with special emphasis on the main areas of uncertainty. Section II contains a brief description of the basic method, with a mathematical model and first-order error analysis being developed in Sections III and IV, respectively. The main conclusions and the requirements for additional analysis are presented in Section V.

II. Differential VLBI

The VLBI technique has been used successfully for
the past five years primarily to study the structures and
positions of compact extragalactic radio sources. For a
strong source, the main limitations on the accuracy achievable
in determining the direction to the source are the result of
(i) instabilities in the frequency standard used at the ob-
serving sites, and (ii) phase fluctuations of the signals
introduced by the propagation medium, mainly the earth's
atmosphere and ionosphere. If several objects in nearly
the same direction are observed simultaneously, these error
sources can either be eliminated or drastically reduced in
their effect on determinations of relative position. The
frequency standard need only be sufficiently stable to
allow fringes to be obtained on the strongest source which
then acts as the standard for comparison with the signals
from the other sources observed simultaneously. The prop-
agation medium effects cancel to the extent that the sig-
nals from the different sources received at a given site pass
through identical paths in the earth's atmosphere and ion-
osphere. Thus the accuracy in relative position determin-
ation can exceed that of "absolute" position determination
by several orders of magnitude.

In observing the quasar 3C279, for example, our VLBI group (Whitney et al. 1971)discovered that its structure was consistent with a two-point-source model; these two "points" were separated by about 1.5×10^{-3} arcseconds and the standard error in the determination of the separation was only 6×10^{-6} arcseconds in the right ascension component. This extremely small error in relative position determination is meaningful because of the small angular separation of the putative two point sources and the consequent high order of cancellation of the propagation medium effects.

We call this technique of relative position determination differential VLBI. We have also applied it successfully to the Apollo 16 Lunar Rover whose position relative to the Lunar Module was monitored throughout the first EVA by use of this method (Shapiro et al. 1972; Counselman et al. 1972). Although the tracking systems were far from optimally arranged for the task and although the radio frequency of the Rover differed from that of the Module by 17 MHz, the final position of the Rover calculated via the differential VLBI technique differed from the estimates of the astronauts by less than 30 m. No accurate intermediate check-points are available for comparison.

The application of differential VLBI to the tracking of the Venus entry probes differs in several important

respects from the Rover-Module case. On the positive side of the ledger, we have the possibilities (i) to choose nearly identical entry probe transmitter frequencies ($\Delta f \lesssim 50 \, kH_3$) to insure that if the different signals pass through the same plasma environment, the latter's effect on phase path will cancel upon differencing; (ii) to design the receiver equipment so that at a given site the local-oscillator signals introduce the same phase noise when mixing with each of the probe signals (the commonality implies that this source of noise will also cancel upon differencing); (iii) to utilize a phase-coherent transponder on at least one of the entry probes; and (iv) to select earth-tracking sites with greater east-west and north-south baseline components. The negative side of the ledger contains more entries: (i) Venus will be about 200 times further away than the moon, causing a corresponding reduction in the accuracy of determination of the projected distance between tracked objects; (ii) the interplanetary medium has a much greater influence on Venus-earth than on moon-earth signals; (iii) Venus has an ionosphere and a thick atmosphere; the moon has virtually none of either; (iv) the tracked Venus probes will move relatively unconstrained through a fluid; the Rover was constrained to adhere to the lunar surface and hence the intrinsic two-dimensional differential VLBI tracking result could be converted to three-dimensional relative position by use of lunar topographic data; (v) the separation between Rover and Module was known at the

start of the VLBI tracking period; for the entry probes
corresponding information will probably not be available
and thus in the latter case only the monitoring of changes
in the (projected) separations of the probes, i.e. only
the monitoring of (projected) velocity differences, will
be possible; and (vi) the thermal environment of the entry
probes will be far less stable than for the Rover and
Module thus tending to cause greater variations in the
transmitter frequencies of the probes.

How does the differential VLBI technique compare
with the straightforward use of a turnaround transponder?
In fact, they are complementary: the transponder supplies
the radial velocity and VLBI the transverse components of
the velocity.* The VLBI approach can be used with either a
transponder or a free-running oscillator to determine the
transverse components; the radial component cannot be use-
fully inferred without a transponder unless the a priori
knowledge of the transmitter frequency is sufficiently ac-
curate. For signal propagation in a vacuum , the trans-
ponder can have an enormous advantage: all other aspects
being equivalent, the error in the determination of radial
velocity will be less than for the differential VLBI determ-

----

*By "radial" we mean parallel to the earth-Venus line.

ination of the transverse components by the ratio of
the VLBI baseline to the distance from the earth to the
source (i.e., by the parallax). For the Venus probes,
this enormous advantage--approximately 2×10^4 in accuracy--
is offset to a great extent by the systematic errors in-
troduced by the propagation medium which largely cancel
in the differential VLBI procedure. One further point
needs to be made here: the differential VLBI procedure
which is needed to cancel these errors yields only the
relative transverse components of velocities for a pair
(or more) of probes; the transponder approach yields the
"absolute" radial velocity for each probe.

We may now address briefly the main problem -- the
determination of the wind speeds in Venus' lower
atmosphere. We distinguish two cases:

(i) Transponders Available on Entry Probes. Here
we would be able to estimate usefully the
velocity vector for all probes from the
ordinary Doppler data. The _a priori_ knowledge
of both the geometry of entry and the terminal
vertical velocity for each probe will most
likely be of sufficient accuracy for this
purpose. The (two-way) effects of the
atmosphere of Venus will introduce uncertainties
well below the   meter-per-second level
unless the geometry is particularly unfavorable.
The wind speeds will be given by the projection
of the velocity vector on the plane normal to
the local vertical at the probe's position.
(We assume that the probe has reached "terminal"

velocity in both the vertical and horizontal directions.) Under these circumstances, the VLBI measurements may not be competitive. But they will still be of interest to provide a check.

(ii) <u>Transponders Not Available in Entry Probes.</u>
Here essentially only the pairwise differences in the probes' velocities projected on the plane normal to the earth-Venus line will be available (except in the unlikely event that the transmitter frequency of one or more of the probes is known very accurately). In general, there is difficulty in separating the contributions of the horizontal velocity components from the vertical components in the projections of the differences. If one of the tracked objects were following a ballistic trajectory (e.g., the bus on a flyby trajectory), then the contribution of the horizontal velocity component of each entry probe could be distinguished. Also, if one of the probes were directed towards the subearth point on Venus, it would be possible to identify part of the velocity projections as being due to winds. If neither of these conditions applies, it appears that models of the terminal descent and appropriate filtering would be required to extract estimates of the wind speeds. Whether such estimates would be useful has not yet been established.

From this qualitative introduction to the problems of the determination of the lower atmospheric wind speeds using differential VLBI, we proceed in the next section to the development of an appropriate mathematical model.

III. Mathematical Model

Our goal here is to develop an algorithm for the determination of wind speeds in Venus' lower atmosphere from VLBI tracking data. Let us begin with the definitions of the relevant geometric quantities. The vector distance $\vec{R}_{ip}$ from the earth-tracking station $\underline{i}$ to the entry probe p can be expressed in a geocentric reference frame as:

$$\vec{R}_{ip}(t, t-\tau_{ip}(t)) \simeq \vec{r}_{ev}(t, t-\tau_{ip}(t)) + \vec{\rho}_p(t-\tau_{ip}(t)) - \vec{r}_i(t), \qquad (1)$$

where $\vec{r}_{ev}$ is the vector distance from the center of mass of the earth to the center of mass of Venus; $\vec{\rho}_p$ is the vector from the center of mass of Venus to the pth probe, $\vec{r}_i$ is the vector from the center of mass of the earth to the ith tracking station, $\underline{t}$ is the time of reception of the signal from the jth probe at the ith tracking station, and τ_{ip} is the time delay between the transmission of a signal from the pth probe and its reception at the ith tracking station.

For the purposes of this section, we shall assume that the signals propagate in vacuum; in Section IV we will consider the medium effects explicitly. Thus, in the approximation of vacuum propagation, the phase delay $\tau_{ip}(t)$ may be found iteratively by means of a simple algorithm:

$$\tau_{ip}(t) = \lim_{n\to\infty} \tau_{ip}^{(n)}(t), \qquad (2)$$

where

$$\tau_{ip}^{(n+1)}(t) = \frac{1}{c} R_{ip}\left(t, t - \frac{1}{c} R_{ip}(t, t-\tau_{ip}^{(n)}(t))\right); \quad n = 0, 1, 2, \ldots, \qquad (3)$$

and

$$\tau_{ip}^{(o)}(t) \equiv \frac{1}{c} R_{ip}\left(t, t - \frac{1}{c} R_{ip}(t,t)\right). \qquad (4)$$

Since the velocities involved are only of the order of $10^{-4}c$, where $\underline{c}$ is the speed of light, one or two iterations will be sufficient to obtain the needed accuracy.

If we assume continuous reception of signals starting from t=0, then the phase $\phi_{ip}(t)$ of the signal received at station $\underline{i}$ from probe p may be written as

$$\phi_{ip}(t) = \phi_{ip}(o) + 2\pi \int_{-\tau_{ip}(o)}^{t-\tau_{ip}(t)} f_p(x)\, dx, \qquad (5)$$

where $f_p(t)$ is the frequency transmitted by probe p at time $\underline{t}$. From the measurements $\phi_{ip}(t)$ we wish to estimate the wind speeds, but in such a manner that we cancel to as high a degree as possible the adverse effects of the propagation medium (which is, however, ignored in the explicit formulation given in this section). By the formation of symmetric double differences, we can insure the tendency to cancel of any potential source of error that is common either to all receivers or to all transmitters.

Before applying this principle, we must consider a means for improvement of the estimate of $f_p(t)$ which is not known accurately a priori. Our results will turn out to

be relatively insensitive to those estimates and so we
will employ sums of the different ϕ_{ip}'z $(i = 1, 2, \ldots)$
to determine each f_p. Since f_p will vary with time in
an unknown manner, we will estimate an average value
$\langle f_p \rangle$ appropriate for each time resolution interval of
interest. Without any important loss in generality, we
may consider this interval to be a constant, T (see
Section IV.). Thus, we may use Eq. (5) to obtain,
successively:

$$
\Delta \phi_{ip}(t_{n-1}, t_n) \equiv \phi_{ip}(t_n) - \phi_{ip}(t_{n-1})
$$

$$
= 2\pi \int_{t_{n-1}-\tau_{ip}(t_{n-1})}^{t_n-\tau_{ip}(t_n)} f_p(x)\, dx \simeq 2\pi \int_{-\frac{T}{2}(1-\dot{\tau}_{ip}(t_{n-\frac{1}{2}}))}^{\frac{T}{2}(1-\dot{\tau}_{ip}(t_{n-\frac{1}{2}}))} f_p\left(y + t_{n-\frac{1}{2}} - \tau_{ip}(t_{n-\frac{1}{2}})\right) dy
$$

$$
\simeq 2\pi T \left(1 - \dot{\tau}_{ip}(t_{n-\frac{1}{2}})\right) \bar{f}_p\left(t_{n-1}, t_n\right) , \qquad (6)
$$

where

$$
t_n \equiv n T \qquad ; \quad n = 0, 1, 2, \ldots , \qquad (7)
$$

$$
t_{n-\frac{1}{2}} \equiv t_{n-1} + \frac{T}{2} \equiv t_n - \frac{T}{2} \qquad , \qquad (8)
$$

$$
\bar{f}_p(t_{n-1}, t_n) \equiv \frac{1}{T(1-\dot{\tau}_{ip}(t_{n-\frac{1}{2}}))} \int_{-\frac{T}{2}(1-\dot{\tau}_{ip}(t_{n-\frac{1}{2}}))}^{\frac{T}{2}(1-\dot{\tau}_{ip}(t_{n-\frac{1}{2}}))} f_p\left(y + t_{n-\frac{1}{2}} - \tau_{ip}(t_{n-\frac{1}{2}})\right) dy, \qquad (9)
$$

$$
\tau_{ip}(t_n) \simeq \tau_{ip}(t_{n-\frac{1}{2}}) + \dot{\tau}_{ip}(t_{n-\frac{1}{2}}) \frac{T}{2} \qquad , \qquad (10)
$$

and where $\dot{\tau}_{ip}(t_{n-\frac{1}{2}})$ signifies the time derivative of the phase delay evaluated at $t=t_{n-1/2}$. If the total number of tracking stations is I, then we consider

$$\langle f_p(t_{n-1}, t_n) \rangle \equiv \frac{1}{I} \sum_{i=1}^{I} \frac{\Delta \phi_{ip}(t_{n-1}, t_n)}{2\pi T(1 - \dot{\tau}_{ip}(t_{n-\frac{1}{2}}))} \quad , \qquad (11)$$

to be the average value of the transmitter frequency f_p over the corresponding receiving time interval (t_{n-1}, t_n) on the assumption that the error in the measurement $\Delta\phi_{ip}$ is independent of $\underline{i}$. If there is a dependence, a more suitable weighting function can easily be substituted. Since $\langle f_p \rangle$ depends on $\dot{\tau}_{ip}$, albeit weakly, the calculations can, and perhaps should, be repeated $\underline{a}$ $\underline{posteriori}$ if more precise values of $\dot{\tau}_{ip}$ become available.

We now return to the task of forming a suitable symmetric double difference. We shall use

$$\frac{1}{cT}\Delta_{ij;pq}^{2s}(t_{n-1}, t_n) \equiv \frac{\Delta\phi_{ip}(t_{n-1}, t_n) - \Delta\phi_{jp}(t_{n-1}, t_n)}{2\pi T \langle f_p(t_{n-1}, t_n) \rangle} - \frac{\Delta\phi_{iq}(t_{n-1}, t_n) - \Delta\phi_{jq}(t_{n-1}, t_n)}{2\pi T \langle f_q(t_{n-1}, t_n) \rangle}, \quad (11)$$

where we defer to the following section a demonstration of the efficacy of this definition. (Here the superscript 2s denotes symmetric double difference.) From Eqs. (1)-(4), (6), and (11) we see immediately that

$$\Delta_{ij;pq}^{2s}(t_{n-1}, t_n) \simeq cT\left[\dot{\tau}_{iq}(t_{n-\frac{1}{2}}) - \dot{\tau}_{ip}(t_{n-\frac{1}{2}}) + \dot{\tau}_{jp}(t_{n-\frac{1}{2}}) - \dot{\tau}_{jq}(t_{n-\frac{1}{2}})\right]$$

$$\simeq \left(R_{iq}^{(n)} - R_{iq}^{(n-1)}\right) - \left(R_{ip}^{(n)} - R_{ip}^{(n-1)}\right)$$

$$+ \left(R_{jp}^{(n)} - R_{jp}^{(n-1)}\right) - \left(R_{jq}^{(n)} - R_{jq}^{(n-1)}\right) , \qquad (12)$$

where

$$R_{ip}^{(n)} \equiv R_{ip}\left(t_n,\, t_n - \tau_{ip}(t_n)\right). \tag{13}$$

To discuss the implications of Eq. (12) conveniently, we shall introduce some approximations. First we introduce the vector $\vec{\rho}_{qr}$:

$$\vec{\rho}_{qr} \equiv \vec{\rho}_p - \vec{\rho}_q \,, \tag{14}$$

which, if the time arguments coincide, represents the vector separation of probes p and q with $\vec{\rho}_{qr}$ extending from q to p. Suppressing time arguments for simplicity, we can expand R_{iq} in terms of R_{ip}:

$$\vec{R}_{iq} = \vec{R}_{ip} - \vec{\rho}_{qp} \,, \tag{15}$$

whence

$$R_{iq} \equiv (\vec{R}_{iq} \cdot \vec{R}_{iq})^{1/2} = (R_{ip}^2 - 2\vec{R}_{ip}\cdot\vec{\rho}_{qp} + \rho_{qr}^2)^{1/2}$$

$$\simeq R_{ip} - \vec{\rho}_{qp} \cdot \hat{R}_{ip} + O\left(\frac{\rho_{qr}^2}{R_{ip}}\right), \tag{16}$$

where $\hat{X} \equiv (\vec{X}/|\vec{X}|)$ signifies a unit vector. The neglected terms in Eq. (16) will in magnitude always be less than $10^{-4}\rho_{qr}$. Using Eq. (16) in Eq. (12) yields

$$\vec{\rho}_{qr} \cdot \left(\hat{R}_{ip}^{(n)} - \hat{R}_{ip}^{(n)}\right) \simeq \vec{\rho}_{qp}^{(n-1)} \cdot \left(\hat{R}_{jp}^{(n-1)} - \hat{R}_{ip}^{(n-1)}\right) + \Delta_{ij;\,p q}^{2S}(t_{n-1}, t_n). \tag{17}$$

By use of further approximations, the expressions for the unit vector differences can be made more perspicuous. Thus,

$$\hat{R}_{ip} \equiv \frac{\vec{r}_{ev} + \vec{\rho}_p - \vec{r}_i}{|\vec{r}_{ev} + \vec{\rho}_p - \vec{r}_i|} \quad , \qquad (18)$$

and

$$|\vec{r}_{ev} + \vec{\rho}_p - \vec{r}_i|^{-1} = \left\{ r_{ev}^2 - 2\vec{r}_{ev}\cdot(\vec{r}_i - \vec{\rho}_p) + (\vec{r}_i - \vec{\rho}_p)\cdot(\vec{r}_i - \vec{\rho}_p) \right\}^{-\frac{1}{2}}$$

$$= r_{ev}^{-1}\left\{ 1 + \left(\frac{\vec{r}_i - \vec{\rho}_p}{r_{ev}}\right)\cdot\hat{r}_{ev} + O\left(\frac{|\vec{r}_i - \vec{\rho}_p|^2}{r_{ev}^2}\right) \right\} , (19)$$

whence

$$\hat{R}_{ip} \simeq \hat{r}_{ev}\left\{ 1 + \left(\frac{\vec{r}_i - \vec{\rho}_p}{r_{ev}}\right)\cdot\hat{r}_{ev} \right\} - \left(\frac{\vec{r}_i - \vec{\rho}_p}{r_{ev}}\right)$$

$$\simeq \hat{r}_{ev} - \frac{1}{r_{ev}}\left\{ (\vec{r}_i - \vec{\rho}_p) - [(\vec{r}_i - \vec{\rho}_p)\cdot\hat{r}_{ev}]\,\hat{r}_{ev} \right\}$$

$$\simeq \hat{r}_{ev} + \frac{1}{r_{ev}}\left\{ \hat{r}_{ev}\times(\hat{r}_{ev}\times[\vec{r}_i - \vec{\rho}_p]) \right\} \quad , \qquad (20)$$

where in the last line we made use of the vector identity:

$$\vec{a}\times(\vec{b}\times\vec{c}) = (\vec{a}\cdot\vec{c})\,\vec{b} - (\vec{a}\cdot\vec{b})\,\vec{c} . \qquad (21)$$

The desired expression for the unit vector difference is therefore

$$\hat{R}_{jp} - \hat{R}_{ip} \simeq \frac{1}{r_{ev}}\,\hat{r}_{er}\times(\hat{r}_{ev}\times\vec{\ell}_{ij}) \quad , \qquad (22)$$

where

$$\vec{\ell}_{ij} \equiv \vec{r}_j - \vec{r}_i \qquad (23)$$

is the baseline vector extending from tracking station i to tracking station j.

What is the physical interpretation of the vector
triple product appearing in Eq. (22)? It is simply the
vector obtained by projecting $\vec{b}_{ij}$ onto the plane normal to
$\hat{r}_{ev}$. In terms of the baseline vectors, we find by sub-
stitution of Eq. (22) into Eq. (17):

$$\vec{\rho}_{ip}^{(n)} \cdot \left[\hat{r}_{ev}^{(n)} \times \left(\hat{r}_{ev}^{(n)} \times \vec{b}_{ij}^{(n)} \right) \right] \simeq \vec{\rho}_{ip}^{(n-1)} \cdot \left[\hat{r}_{ev}^{(n-1)} \times \left(\hat{r}_{ev}^{(n-1)} \times \vec{b}_{ij}^{(n-1)} \right) \right] + r_{ev}^{(n-1)} \Delta_{ij,pq}^{is}(t_{n-1}, t_n),$$

$$(24)$$

where we also neglect the very small difference between $r_{ev}^{(n)}$
and $r_{ev}^{(n-1)}$. So long as the vectors $\hat{r}_{ev} \times (\hat{r}_{ev} \times \vec{b}_{ij})$ for the
different pairs (ij) are not parallel, Eq. (24) will allow
the changes in the vector separation of the probes, projected
onto the plane normal to the earth-Venus line, to be followed
during the period of continuous tracking of the probe pairs.
The actual projected vector separation, as opposed to changes
in it, cannot be determined from these data alone because the
initial such separation--at the time simultaneous tracking
commences--is uncertain due to the fringe ambiguity. Because
of the narrow band of the emissions from the probes, the pro-
jected separation of the probes will only be determined to
within the equivalent of an integral number of fringes. A
single fringe corresponds, for the typical VLBI baselines
under consideration, to a projected distance at Venus of about
3 km. This ambiguity can be eliminated by simultaneous use of

a shorter baseline interferometer pair for which the fringe
spacings in the two orthogonal directions, in the plane normal
to the earth-Venus line, are larger than the corresponding
a priori uncertainties. This elimination is useful for
establishing the geometry.

In particular, our main object is to determine wind speeds.
To this end, we develop the expressions for the components of
the velocity difference $\dot{\vec{\rho}}_{\dot{v}p}^{(n)}$ on the plane normal to $\vec{r}_{ev}$
(a dot signifies differentiation with respect to time). For
convenience, we ignore the superscript (n), assume we have a
continuous determination of the projection of $\dot{\vec{\rho}}_{\dot{v}p}(t)$, and
define

$$\dot{\vec{\rho}}_{\dot{v}p}^{\perp}(t) \equiv (\dot{\vec{\rho}}_{\dot{v}p}\cdot\hat{e}_1)\,\hat{e}_1 + (\dot{\vec{\rho}}_{\dot{v}}\cdot\hat{e}_2)\hat{e}_2 \quad , \qquad (25)$$

where the unit vectors $\hat{e}_1$ and $\hat{e}_2$ are mutually orthogonal and
lie in the plane normal to $\vec{r}_{ev}$. Since the relevant portion
of the probes' descent through Venus' atmosphere occurs on
a time scale short compared to a day, we ignore here the time
dependences of $\vec{b}_{ij}$ and $\vec{r}_{ev}$.* The vectors $\hat{e}_i$ $(i=1,2)$ can be
defined, for example, by

$$\hat{e}_{p1} \equiv \frac{\hat{r}_{ev}\times(\vec{\rho}_p\times\hat{r}_{ev})}{|\hat{r}_{ev}\times(\vec{\rho}_p\times\hat{r}_{ev})|} \quad , \qquad (26)$$

$$\hat{e}_{p2} \equiv \frac{\hat{r}_{ev}\times\vec{\rho}_p}{|\hat{r}_{ev}\times\rho_p|} \quad , \qquad (27)$$

where $\hat{e}_{p1}$ is parallel to the projection of $\vec{\rho}_p$ and $\hat{e}_{p2}$ is

---

*These and other mathematical approximations would, of course,
not be made in a realistic model to be used in an actual
analysis of data.

normal to this projection. We also ignore the slight change in direction of $\vec{\rho}_P$ during final descent insofar as this change affects $\hat{e}_{px}$. Both components of $\vec{\rho}_{qr}^{\perp}$ are determined since we assume that the projections of the various baseline vectors $\vec{b}_j$ span the plane normal to $\vec{r}_{ev}$.

How may we estimate wind speeds from this measured vector function $\vec{\rho}_{rq}^{\perp}$? First, we assume that the horizontal velocity of each probe is equal to that of the local wind (see *Section IV*). Second, we decompose the velocity of each probe into its vertical and horizontal parts and project each onto the plane normal to $\vec{r}_{ev}$ to determine their effects on the measured vector function. Thus we set

$$\vec{\dot{\rho}}_P(t) = \vec{\dot{\rho}}_P^{V} + \vec{\dot{\rho}}_P^{H} , \qquad (28)$$

where

$$\vec{\dot{\rho}}_P^{V} \equiv (\vec{\dot{\rho}}_P \cdot \hat{\rho}_P)\hat{\rho}_P , \qquad (29)$$

$$\vec{\dot{\rho}}_P^{H} \equiv \hat{\rho}_P \times (\vec{\dot{\rho}}_P(t) \times \hat{\rho}_P) , \qquad (30)$$

and where we again ignore the variation in $\vec{\rho}_P$ during descent in its effect on the unit vector $\hat{\rho}_P$. In terms of these definitions and similar ones for the qth probe, we have:

$$\vec{\dot{\rho}}_{qp}^{\perp} \equiv \vec{\dot{\rho}}_p^{\perp} - \vec{\dot{\rho}}_q^{\perp} = \left[(\vec{\dot{\rho}}_p^{H} + \vec{\dot{\rho}}_p^{V}) \cdot \hat{e}_{p1} \right] \hat{e}_{p1} + (\vec{\dot{\rho}}_p^{H} \cdot \hat{e}_{p2}) \hat{e}_{p2}$$

$$- \left[(\vec{\dot{\rho}}_q^{H} + \vec{\dot{\rho}}_q^{V}) \cdot \hat{e}_{q1} \right] \hat{e}_{q1} - (\vec{\dot{\rho}}_q^{H} \cdot \hat{e}_{q2}) \hat{e}_{q2} .$$

$$(31)$$

From this general expression, we can examine some special cases:

(1) One of the objects being tracked has a transponder and is not passing through the lower atmosphere. Since the trajectory for this object, say $\underline{q}$, can be reconstructed from the Doppler data, the coefficient of $\hat{e}_{p_L}$ can be isolated and will yield directly the projection of $\vec{\rho}_p^H$.

(2) Both objects being tracked are passing through the lower atmosphere, but the unit vector $\hat{\rho}_p$ and the velocity component parallel to $\vec{r}_{ev}$ are known for each probe from transponder data (or, equivalently--if it were possible, from sufficiently accurate a priori knowledge of the transmitter frequency for each probe). In this instance, the differential VLBI data can be used to yield the time dependence of the vector difference between the projections of the horizontal velocity components of the probes onto the plane normal to $\vec{r}_{ev}$. This function can be compared with the corresponding estimate obtained from the trajectory reconstruction.

(3) No data other than the differential VLBI data are available. Here, there are a number of subcases

that should be mentioned. First, assume $\vec{\rho}_{P}, \vec{\rho}_{\delta},$
and $\vec{r}_{ev}$ are coplanar. We would then have
$\hat{e}_{p'} = \pm\ \hat{e}_{\delta'}$ and $\hat{e}_{p\iota} = \pm\ \hat{e}_{\delta\iota}$. The com-
bined coefficient of $\hat{e}_{p\iota}$ and $\hat{e}_{\delta\iota}$ in
Eq. (31) would therefore yield directly the
projection of the horizontal velocity differ-
ence. One can then apportion horizontal vel-
ocities between the probes in a variety of
ways consistent with the measured function
and with "plausibility." If $\hat{\rho}_{P}, \hat{\rho}_{\delta},$ and $\vec{r}_{ev}$
are not coplanar, the differences of the pro-
jected horizontal velocity components do not
separate. Several alternatives then exist:
(i) admit defeat; (ii) arrange to have one
of the probes enter at the subearth point so
that $\vec{\rho}_{r}^{V}$ would have no component in the plane
normal to $\vec{r}_{ev}$, thus allowing the coefficient
of $\hat{e}_{\delta\iota}$ to depend only on the projections of
horizontal velocity components; or (iii) use
all other available data to estimate $\vec{\rho}_{r}^{V}$ and
$\vec{\rho}_{\delta}^{V}$ so that the observed function $\vec{\rho}_{\delta P}^{\iota}$ can
be used to delimit the differences in the pro-
jected horizontal velocities.

(4) Null results are obtained. Suppose we get a null value for the difference in projected horizontal velocities. What other possibilities, aside from the absence of winds, would be consistent with such a result? Unless the $\vec{\rho}_h{}'$ are normal to $\vec{r}_{ev}$--a very unlikely event-- the only other possibilities are either a cancellation of the projections from the two probes or an alignment of the projections of $\vec{\rho}^H$ and $\vec{\rho}^V$ for each probe and a consequent apparent absence of $\vec{\rho}^H$. The cancellation might come about, for example, if the winds were east-west at a constant speed, independent of height, and if the probes entered symmetrically about the meridian of the subearth point.

In summary, we have developed a mathematical model to show that in most circumstances the differential VLBI measurements will yield information on the wind speeds in Venus' lower atmosphere. But the crucial question concerns whether or not such information is useful. That question is addressed in the following section.

IV. Error Analysis

For a proper assessment of this application of differential VLBI, we must investigate a large number of possible sources of error. It has not been possible in the limited time available to carry out as complete an investigation as is required. Thus, we shall simply list many of the questions which need answering, followed in turn by the status of our analysis of each:

1. What is the basic resolution capability of differential VLBI with respect to the entry probes?

2. What are the limitations imposed by:

   i. lack of clock synchronization between the various receiving sites on earth;

   ii. the receiver systems;

   iii. the atmosphere of Venus;

   iv. the atmosphere of the earth;

   v. the ionospheres of Venus and the earth, and the interplanetary medium;

   vi. instability of the transmitter frequency;

   vii. uncertainty in the geometry of entry for the probes or in the trajectory of the bus if the latter is used as a reference?

3. What are the optimum configurations of the probes with respect to positions and times of entry?

1. To determine the basic resolution capability, we note that the weakest signals will be from the miniprobes which will transmit about 1 w of effective radiated power when near the surface of Venus. If the bandwidth of this signal is no more than 50 Hz (probably a gross upper bound), then the flux at the earth will be no less than about 30 FU (1 FU = 10^{-26} w/m^2-Hz). For the antenna systems that might be used in the experiment--Goldstone, Madrid, Arecibo, Haystack, and Johannesburg--the fringe phase uncertainty, due solely to system noise, would be under 1° after only one or two seconds of integration (see, also, 2.ii below). Such a fringe phase error corresponds to a displacement uncertainty at Venus of about 6 m for this S-band signal with a projected baseline of 4000 km and an earth-Venus separation of 0.5 a.u. Thus average projected velocity differences could be measured over a time interval $\underline{t}$ with an uncertainty of only about 10 t^{-1} m/sec, where $\underline{t}$ is in seconds, if the system noise were the only source of uncertainty. We may compare this resolution with the time required for the entry probes to acquire the horizontal speed $\vec{v}_w$ of the wind. As a crude model, consider the probe to be spherical of radius R and average

density ρ . Then, if we neglect the density of the atmosphere relative to that of the probe, the probe's horizontal acceleration a_H will obey:

$$a_H = K \left(v_w - v_H \right) , \qquad (32)$$

whence its velocity v_H will be given by

$$v_H = v_w \left(1 - e^{-K(t-t_o)} \right) , \qquad (33)$$

where the time constant K^{-1} is

$$K^{-1} = \frac{2 R^2 \rho}{9 \eta} , \qquad (34)$$

with η being the viscosity. Since the terminal vertical velocity v_V is given approximately by

$$v_V \simeq K^{-1} g , \qquad (35)$$

we have $K^{-1} \simeq 5$ sec for $v_V \simeq 50$m/sec, etc.[*] The required VLBI integration time thus appears well matched to the time scales in which the probes reflect the local wind speeds in the lower atmosphere.

2.i.   The lack of precise clock synchronization between the various receiving sites should introduce no detectable error if the data are properly taken. With the signals from each object tracked being sampled simultaneously, the clock error cancels completely upon differencing. In effect, the strong signal, say from the bus or main probe, acts as the clock for the weaker signals from the miniprobes. A large epoch offset of the station clock from one site relative to that from another only increases the set of trial times that

---

[*] Here g is the acceleration of gravity on the surface of Venus.

need be introduced in the usual cross-correlation procedure used to search for fringes. However, even this minor problem disappears if advantage is taken of the presence of the carrier signal from each source as we explain below.

2.ii. The receiver system, if properly configured, also need introduce no detectable errors. We require here that the different local-oscillator signals, used at a given site to heterodyne the radio-frequency signals from the various objects being tracked, all be derived from the same frequency standard and, insofar as possible, from the same L.O. chain elements. The purpose of these strictures is to insure that almost all of the phase noise of the heterodyne signals are common to the receiver chains for all tracked objects. The common phase noise thus introduced will then cancel upon differencing. The residual (non common) phase noise can probably be reduced without much difficulty to the order of 1°.

In connection with the receiver system, we also note that the presence of a carrier signal--lacking in the usual celestial sources involved in VLBI experiments--allows the tape recording of the heterodyned signals and subsequent cross correlation to be eliminated. If the carrier signal from each probe is sufficiently stable, it can be tracked with a suitable phase-locked loop (of third order, if necessary,

to follow drifts in transmitter frequency) and only the usual counted-Doppler values need be recorded. These samples can be incorporated directly into the double-difference observable defined in Section III. We must still insure that the samples for each tracked object are obtained simultaneously, or very nearly so, to insure that the clock synchronization errors cancel.

2.iii. The atmosphere of Venus can be expected to introduce sizable phase variations in the signals received at a given site from a given tracked object. The one-way electrical path length of the Venus atmosphere is about 300 m in the zenith direction. However, the phase variations introduced will be virtually identical in their effects on the signals received at each of the earth-based tracking stations. The geometric beams from a given entry probe to each of the tracking stations are separated by about 1 m at an altitude of 20 km. The Fresnel zone at that altitude for these S-band signals measures about 70 m across. Since the overlap is almost complete, this error source will largely vanish in the symmetric differencing process. The residual phase noise will be due to the small crescent-shaped non-overlap regions, separated by about 70 m at a 20 km altitude and by less at lower altitudes. This noise will depend on the spatial spectrum of the atmospheric inhomogeneities and on the wind speeds. No attempt has yet

been made to estimate this contribution quantitatively.

2. iv. The earth's atmosphere introduces far less severe phase fluctuations since it has a zenith electrical path length of less than 3m--two orders of magnitude smaller than for Venus. The almost complete overlap of the beams entering a given antenna aperture from the various entry probes insures a high-order of cancellation of the atmospheric effects in the differencing procedure. No quantitative estimate has yet been made of the residual noise, although relevant noise statistics are available. In summary, the Venus atmospheric effects tend to cancel because of the differencing of the signals received at the different receiving sites whereas the corresponding effects of the earth's atmosphere tend to cancel because of the differencing of the signals from the various probes. The beauty of the symmetric double-difference technique is thus apparent.

2.v. The effect of the charged particles along the propagation paths--equivalent to a change in electrical path length of less than 15 m--will also tend to cancel in the double difference. But here there are several important differences from the atmosphere case: (a) The path separations midway between earth and Venus are about 2000 km, compared to a Fresnel zone size of about 100 km; (b) The ionospheres have peak densities at altitudes of hundreds of kilometers; and (c) The lack of exact equality

among the transmitter frequencies will prevent complete cancellation of plasma effects due to dispersion. To insure that the frequency differences Δf cause corresponding variations in phase path of no more than $1°$, it is necessary that $\Delta f \lesssim 20\,kHz$. If the charged-particle contributions can be modelled from other data to within 40%, then this restriction can be relaxed to $\Delta f \lesssim 50\,kHz$. The lack of cancellation due to non-overlap of the various paths again will depend on the spatial and temporal spectra of the inhomogeneities. And again no attempt has yet been made to estimate quantitatively this source of residual phase error.

It may, in fact, be possible to solve for the above propagation medium effects if all probes can be tracked simultaneously from more than three earth-based antenna sites. The multiplicity of paths provides redundancy which may be used in a suitable filtering scheme to eliminate all medium effects. (We assume that the differences in transmitter frequencies introduce negligible dispersion.) The analysis of this multi-probed many-sited situation has been started, but not completed.

2.vi. Variations in the frequencies of the transmitters make difficult their calibration by means of the one-way Doppler values. Errors in this calibration will tend to introduce asymmetries into the double-difference observable with the consequence, for example, that the propagation

medium effects will not cancel as completely. An a priori
knowledge of these frequencies, accurate to 1 part in 10^8,
would certainly be sufficient to eliminate this source of
error. Whether or not a knowledge of them to 1 part in
10^6--a more realistic figure--will be sufficient is un-
certain. A detailed analysis of this aspect is in progress
but has not been completed. With turn-around transponders,
the problem all but disappears.

2.vii. Uncertainties in the geometrical configuration
of the entry probe vectors $\vec{\rho}_P$ (see Section III) will
affect the interpretation of the data in terms of wind
speeds. Similarly, uncertainties in the velocity vector
of the bus, if it is used as a reference, will introduce
interpretation difficulties. Although no quantitative
estimates have been made, the trajectory reconstruction
for the bus should be sufficiently accurate with Doppler
errors at the 1 mm/sec level or below. Hopefully, the
medium effects and the unknown harmonics of Venus' grav-
itational field won't vitiate this conclusion. With the
bus providing a reference, the small uncertainties in the
entry probe geometry will be of little consequence; such
will not be the case if only the several miniprobes are
tracked simultaneously. But then other problems loom larger,
as mentioned in Section III.

3. It would be best to have the bus tracked simultaneously with each entry probe (no entry occultations allowed during this period!) and to have the trajectory of the bus passing far enough from Venus to minimize the effects of the higher harmonics of the gravity field. Arrayed against this requirement will be the reduction in cancellation of propagation medium effects that accompanies an increase in angular separation of the targets. If the bus is unavailable, then wind speeds seem to be easiest to isolate (see Section III) if one of the simultaneously tracked entry probes is directed towards the subearth point on Venus. Again, the quantitative advantages have not been analyzed.

V.   Conclusions

We conclude that wind speeds in the lower atmosphere of Venus can be detected via differential VLBI observations of the entry probes. The uncertainty in the wind speed determination can probably be kept below $100\ t^{-1}$ m/sec, where $t > 1$ is the time resolution in seconds, provided that:

(1) the residual effect of the propagation medium on the symmetric double-difference observable can be be kept below about 10° of phase at S-band; and

(2) the transponded signals from the bus, on an exo-atmospheric trajectory, are available as a reference.

Condition (1), which is crucial, is unfortunately not buttressed by a prima facie case. The loopholes left, discussed in Section IV, are related to the effects of the non-overlap regions of the propagation paths and the instabilities of the transmitters. (We assume, in addition, that the differences in transmitter frequencies are no more than about 50 kHz .) If the signals from the bus were not available as a reference, the main probe with its transponder could serve the same function with a loss in accuracy that would probably not be too severe but that hasn't been estimated quantitatively. If only the miniprobes--without transponders--can be tracked simultaneously, the situation looks grim because of the difficulty in separating the contributions of the vertical

and horizontal velocity components to the observed pro-
jections on the plane normal to the earth-Venus line.
Unless the vertical velocity components can be modelled
accurately, the only apparent solution in this circumstance
is to have one of the miniprobes directed towards the
subearth point.

Of course, if a transponder were available on each
probe, all of these problems would fade away. The recon-
struction of the horizontal probe velocity from the pro-
jection of the total velocity vector along the earth-Venus
line should be reasonably accurate even after allowance for
uncertainties in the entrance geometry, the terminal vertical
velocity, and the (two-way) effects of Venus' atmosphere on
the observed Doppler shift.

The main conclusion to be drawn on the potential of
differential VLBI, per se, for the determination of wind
speeds is that, despite this mass (mess?) of verbiage, much
work remains to be done to assure a proper assessment.

References

1. A.R. Whitney, I.I. Shapiro, A.E.E. Rogers, D.S. Robertson, C.A. Knight, T.A. Clark, R.M. Goldstein, G.E. Marandino, and N.R. Vandenberg, _Science_ 173, 225 (1971).

2. I.I. Shapiro, C.C. Counselman, and H.F. Hinteregger, "Lunar Rover Tracking Via VLBI", Report prepared for the Manned Space Flight Net, Goddard Space Flight Center, 1971.

3. C.C. Counselman, H.F. Hinteregger, and I.I. Shapiro, "Astronomical Applications of Differential Interferometry", to be submitted to _Science_.

SCIENCE

Astronomical Applications of Differential Interferometry

C. C. Counselman, III, H. F. Hinteregger and I. I. Shapiro

Astronomical Applications of Differential Interferometry

Abstract. *Intercomparison of radio signals received simultaneously at several sites from several sources with small mutual angular separation provides a powerful astrometric tool. Applications include tracking the Lunar Rover relative to the Lunar Module, determining the moon's libration, measuring winds in Venus's lower atmosphere, mapping Mars radiometrically, and locating the planetary system in an inertial frame.*

In most applications of very-long-baseline interferometry (VLBI) the most serious limitations on the accuracy of the results are imposed by unknown, variable phase errors introduced by both the neutral atmosphere and the ionosphere above the receiving sites, and by fluctuations in the rates of the oscillators that provide phase references at the separate sites. These limitations may be largely removed in differential measurements, in which signals received simultaneously from different radio sources located close together in the sky are compared. If atmospheric and independent oscillator phase shifts affect observations of each source equally, their effects will cancel when differences between observations are examined. In this report we discuss several scientific applications of differential interferometry (*1*), as well as the actual tracking of the Lunar Rover performed during the Apollo 16 mission.

Because differential interferometry involves taking differences not only between receiving points but also between transmitting points, it follows that any potential source of error will cancel if it is common either to all receivers or to all transmitters. This simple principle will be shown to have important consequences for astronomical measurements. One such consequence relates to observations of artificial transmitters for which the carrier frequency may be uncertain and variable. Noninterferometric one-way Doppler tracking of such objects is ordinarily of little use because changes in the received frequency due to the Doppler shift cannot be distinguished from changes in the frequency of the transmitter itself. In interferometry, however, transmitter (and any other) frequency changes that appear equally at all receivers have no direct effect on the ability of the interferometer to determine relative angular positions. In fact, artificial radio sources make particularly convenient objects for interferometry because conventional Doppler counting techniques can be used to keep track of the phase of the carrier signal received at each site. Wide-bandwidth group-delay interferometry also may be done efficiently with artificial sources if the carrier wave is suitably modulated, for example, with a pseudorandom wave form of the kind often employed for two-way radar ranging (*2*). As in the case of one-way Doppler tracking, one-way radar ranging is ordinarily useless if either or both of the transmitter and receiver time bases are unstable. But for either phase-delay or group-delay observables, the effects of transmitter instability cancel when the difference is taken between receiving sites (thus forming an interferometric observable), and the ef-

fects of receiver instability cancel when the difference is taken between a pair of transmitters (forming a differential interferometric observable).

We shall now discuss some of the potential scientific applications of differential interferometry. First, however, we describe one technical application already successfully carried out: Earth-based tracking of the Apollo 16 Lunar Rover relative to the Lunar Module. Three tracking stations (*3*) were employed so that two independent baselines were formed. Thus, two components of the motion of the Rover relative to the Module were determined from the changes in phase of the two differential interferometric observables. From the initial separation of the Rover and the Module and the constraint that the Rover remained on the lunar surface, it was possible to determine its entire path (Fig. 1). After a traverse of over 4 km, the final position computed from these data differed from the actual position by about 30 m, or about 0.015 arc second at the distance of the moon (*4*). The main source of error was relative phase drift between the two receivers (one each for the Rover and the Module) used at each site in this trial experiment. In an operational system this error would be eliminated by using a single receiver for both signals. The basic technique appears capable of reducing tracking errors to the meter level, a limit imposed by unmodeled lunar topography.

A related scientific application involves the accurate determination of the moon's libration by monitoring simultaneously from several tracking stations the ALSEP (*5*) telemetry transmitters located at three well-separated sites, such as those of Apollo 14, Apollo 15, and Apollo 16. Here, because the ALSEP's are fixed on the lunar surface,
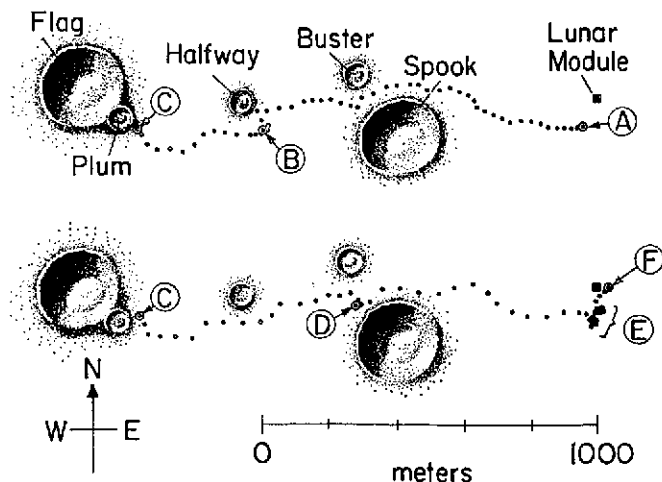

Fig. 1. The path of the Apollo 16 Lunar Rover is shown as determined by Earth-based differential interferometric tracking on 21 April 1972. Individual dots mark the positions obtained at 20-second intervals, beginning at 20:52:40 U.T. from point *A*. Craters given names by the astronauts are included for reference, although their locations are known only approximately. The Rover was stopped at point *B* for 6^m20^s, at *C* for $1^h9^m40^s$, and at *D* for 27^m0^s; several brief stops were made at *E*. At 23:03:40 our tracking indicated that the Rover had stopped finally at *F*, 30 m east of the Lunar Module; the Rover had actually parked at the Module. Some of this error may reflect a corresponding error in the assumed starting position, *A*. However, tracking data obtained while the Rover was known to be stopped occasionally showed systematic drifts as large as 2 or 3 cm/sec (see text). Random noise was less than 1 m. At all times during the traverse, position readings from the navigation system on board the Rover agreed within 100 m (approximately the limit of precision of the onboard system) with these differential interferometric tracking results.

their relative positions must be determined by monitoring changes in the phases of the differential interferometric observables over a sizable fraction of a day. Lunar libration causes these apparent positions to vary over the course of a month, and longer. The differential nature of the observable sharply reduces the effects of errors in the lunar ephemeris, tracking station coordinates, and so forth, and should yield at least an order of magnitude improvement in our knowledge of the libration [present uncertainty about 10 seconds of selenocentric arc (6)].

Differential interferometric tracking of planetary probes, landers, and orbiters will yield results in many cases more accurate than can be obtained from tracking satellites of the earth. This seemingly paradoxical conclusion follows because the usual limitation is set not by signal strength but by systematic effects of the atmosphere and ionosphere, and sometimes by receiving-system phase instabilities. These effects cancel in the differential interferometric observable. A planetary application of differential interferometry which is analogous to, but more complicated than, the Lunar Rover–Lunar Module situation involves tracking a number of small probes descending simultaneously into Venus's atmosphere (7). By differential tracking of the free-falling probes relative to a parent spacecraft it should be possible to detect horizontal winds at the level of a few meters per second. Differential interferometry could also aid in the interpretation of occultation data (8). Additional applications of differential interferometry to both orbiters and landers are too numerous to be elaborated here; for example, improved estimates of the planet's gravity model parameters, rotation vector, and landing site or orbit parameters may be expected [see, for example, (8)]. Whenever the planet passes close to the direction of an extragalactic radio source, differential interferometry may be used to determine the earth-planet direction relative to that of the source to about 0.001 arc second. Such measurements could be used to determine precisely the orientation of planetary orbits with respect to an inertial frame and, for example, to monitor the perihelion precessions to further test general relativity. For ground-based radiometric mapping of the terrestrial planets, differential interferometry can overcome the effects of instrumental, atmospheric, and ionospheric phase drifts, which limit the application of aperture-synthesis tech-

niques. A phase reference could be provided, for example, by the specular echo of a radar signal sent at the appropriate frequency (9). Such mapping appears especially important for Mars where the distribution of small amounts of surface water (or ice) might be discernible from millimeter-wavelength observations (10).

In summary, the technique of differential interferometry seems capable of solving a wide range of astronomical problems.

C. C. COUNSELMAN, III
H. F. HINTEREGGER
I. I. SHAPIRO
Department of Earth and Planetary Sciences, Massachusetts Institute of Technology, Cambridge 02139

References and Notes

1. This principle has already been applied in lunar and planetary radar experiments, in mapping the relative positions of closely spaced sources in the sky, and in the detection of the differential gravitational deflection of radio signals by the sun. Our discussion concerns new applications, especially ones in which a carrier signal is available from each source.
2. A matched-filter receiver could then be used to estimate the delay at each site, in the same way as for two-way ranging. See, for example, J. V. Evans and T. Hagfors, Eds., *Radar Astronomy* (McGraw-Hill, New York, 1968), pp. 500–509. The value obtained at one site would not, by itself, be significant, but the difference between sites would. Phase delay could be measured simultaneously with group delay if a Doppler counter were also available at each site. In addition to not requiring direct recording of the signals for VLBI, artificial sources have an enormous signal-to-noise advantage over natural sources because they are coherent.
3. These stations (in Madrid, Spain; on Ascension Island; and at Cape Kennedy, Florida) belong to the Spacecraft Tracking Data Network (STDN) of the National Aeronautics and Space Administration (NASA), and are managed by Goddard Space Flight Center.
4. A detailed discussion of the algorithms used is presented by us in "The STDN Metric Tracking Performance Apollo 16 Final Report," No. X832-72-203, available from the Librarian, Goddard Space Flight Center, Greenbelt, Maryland 20771.
5. ALSEP is an acronym for Apollo Lunar Surface Experiments Package.
6. Observations of the ALSEP's to determine the lunar libration are now being considered by the STDN (3) (I. Salzberg, personal communication).
7. Space Science Board, *Venus, Strategy for Exploration* (National Academy of Sciences, Washington, D.C., 1970), pp. 33–34.
8. W. H. Michael, Jr., D. L. Cain, G. Fjeldbo, G. S. Levy, J. G. Davies, M. D. Grossi, I. I. Shapiro, G. L. Tyler, *Icarus* 16, 57 (1972).
9. This application of differential interferometry is similar to the phase-calibration technique used for unambiguous radar delay-Doppler mapping of Venus by A. E. E. Rogers and R. P. Ingalls [*Science* 165, 797 (1969)].
10. C. Sagan and J. Veverka, *Icarus* 14, 222 (1971).
11. The Lunar Rover tracking results shown here resulted in part from the programming and related aid performed at Goddard Space Flight Center by E. S. Shaffer and D. Shnidman of the Bendix Company. Invaluable support was also provided by the Metric Data Branch at Goddard, and especially by the Tracking Data Evaluation Section. The Lunar Rover tracking project was headed by I. Salzberg.

19 June 1972

SCIENCE

Venus: Radar Determination of Gravity Potential

Irwin I. Shapiro, Gordon H. Pettengill, Gary N. Sherman
Alan E. E. Rogers and Richard P. Ingalls

Venus: Radar Determination of Gravity Potential

Abstract. *We describe a method for the determination of the gravity potential of Venus from multiple-frequency radar measurements. The method is based on the strong frequency dependence of the absorption of radio waves in Venus' atmosphere. Comparison of the differing radar reflection intensities at several frequencies yields the height of the surface relative to a reference pressure contour; combination with measurements of round-trip echo delays allows the pressure, and hence the gravity potential contour, to be mapped relative to the mean planet radius. Since calibration data from other frequencies are unavailable, the absorption-sensitive Haystack Observatory data have been analyzed under the assumption of uniform surface reflectivity to yield a gravity equipotential contour for the equatorial region and a tentative upper bound of 6×10^{-4} on the fractional difference of Venus' principal equatorial moments of inertia. The minima in the equipotential contours appear to be associated with topographic minima.*

Present knowledge of the surface of Venus rests largely on the results of radar observations. Perhaps the most striking fact to emerge has been the retrograde direction of Venus' spin and its apparent resonance with the relative orbital motions of the earth and Venus (*1*). The earth could have captured Venus' spin in this resonance only through the action of a gravitational torque on a substantial axial asymmetry in Venus' mass distribution (*2*). Heretofore, no measurement of this asymmetry has been possible. The main purpose of this report is to demonstrate that future radar observations can be used to determine equipotential contours of Venus' gravity field and, hence, to estimate the axial asymmetry of its mass distribution. A preliminary contour for the equatorial region and a concomitant bound on the axial mass asymmetry—based on past radar observations not made explicitly for this purpose—is also included.

How can radar data be sensitive to the gravity field of Venus? A direct sensitivity seems almost unthinkable. But an indirect intermediary exists, namely, the thick, carbon-dioxide-dominated atmosphere of Venus. Because this atmosphere absorbs X-band (approximately 8000 Mhz) radio radiation strongly and, for example, S-band (approximately 2000 Mhz) radiation hardly at all, we can infer surface heights relative to a particular pressure contour from a comparison of radar cross sections measured at the two frequencies, since the intrinsic reflectivity of the surface itself should not, in general, vary sharply with frequency (*3*). The use of a third frequency would allow a more precise separation of atmospheric from surface reflectivity effects on cross section. The pressure contours can then be related to the mean planet

radius with the aid of measurements of round-trip radar echo time-delays, which allow the absolute surface heights to be determined (*4*). Gravity equipotential contours will coincide with pressure contours under conditions of hydrostatic equilibrium in the atmosphere (*5*). From such a contour, the gravitational torque exerted by the earth can be estimated.

Now we develop this basic idea quantitatively. Since at present its application is restricted to the equatorial regions traversed by the subradar point of earth-based observations, we confine our analysis to that situation. The possibilities for extension to high latitudes and for the use of radars on Venus orbiters are discussed briefly in the last part of the report.

The radar cross section $\sigma(\lambda,\phi)$ per unit surface area at the subradar point can be written as

$$\sigma(\lambda,\phi) = \sigma_0(\lambda,\phi)\exp[-2\tau(\lambda,\phi)] \quad (1)$$

where

$$\tau(\lambda,\phi) = \int_{h(\phi)}^{h_{max}} \kappa(h,\lambda)\,dh \quad (2)$$

with λ being the wavelength of the radar signals, ϕ the longitude of the subradar point (we suppress θ, the latitude dependence), σ_0 the intrinsic cross section per unit area of the observed region of the surface, τ the opacity (optical depth) of the atmosphere, κ the absorption coefficient for radio waves, h the height of the reflecting region relative to a reference pressure contour, and h_{max} the altitude above which absorption can be neglected. We define the reference contour in terms of a reference longitude ϕ_0 such that $h(\phi_0) \cong 0$. The factor of 2 multiplying τ in Eq. 1 accounts for the two-way passage of the radio waves through Venus' atmosphere. The coefficient, κ,

is given approximately by the semi-empirical formula (*6*)

$$\kappa(h,\lambda) \simeq \frac{1.57 \times 10^{-2}P^2(h)}{\lambda^2[T(h)/273]^3}\,\text{km}^{-1} \quad (3)$$

where P is the pressure in atmospheres, T the temperature in degrees Kelvin, and λ the wavelength in centimeters. Since the absorption is important only in the lower atmosphere, we may use the approximate temperature-pressure relation (*7*)

$$\frac{P(h)}{P(0)} \simeq \left[\frac{T(0) - Lh}{T(0)}\right]^k \quad (4)$$

in the evaluation of τ. Here $h = 0$ refers to the reference pressure contour; $L \simeq 9°K$ per kilometer is the lapse rate, assumed constant· and $k = \mu g/RL \simeq 5.3$ is the polytropic index, with μ the mean molecular weight of the atmosphere, g the acceleration of gravity, and R the gas constant. From Eqs. 1 through 4 we obtain

$$\frac{\sigma(\lambda,\phi)}{\sigma(\lambda,\phi_0)}\frac{\sigma_0(\lambda,\phi_0)}{\sigma_0(\lambda,\phi)} \simeq$$
$$\exp\left(-\frac{\kappa(0,\lambda)T(0)}{(k-2)L}[(1-\frac{Lh}{T(0)})^{2(k-2)} - 1]\right)$$
$$\simeq \exp[2\kappa(0,\lambda)h] \quad (5)$$

where the last relation is valid only for $h << [T(0)/L] \simeq 90$ km. Since h does not seem to vary by more than about ± 4 km (*4, 8*), the expansion used in the last part of Eq. 5 will be in error by less than 15 percent. Hence, for expository purposes, we confine discussion to the simplified form. Solving for h then yields

$$h(\phi) \simeq \frac{1}{2\kappa(0,\lambda)}\ln\left[\frac{\sigma(\lambda,\phi)}{\sigma(\lambda,\phi_0)}\frac{\sigma_0(\lambda,\phi_0)}{\sigma_0(\lambda,\phi)}\right] \quad (6)$$

Assuming that the multiple-frequency observations provide the ratios σ/σ_0, how may we use the resultant values of $h(\phi)$ to determine the height variation of the reference contour with respect to the mean surface radius, ρ? From the value of the echo time-delay, measured simultaneously with the cross section, we can infer the height, h', of the reflecting region above the mean radius (*4*). Thus, the height, h'', of the reference pressure contour above the mean radius is given by

$$h'' = h' - h \quad (7)$$

The function $h''(\phi)$ defines a gravity equipotential contour over the equatorial region under conditions of atmospheric hydrostatic equilibrium (*5*). If the contribution of the centrifugal acceleration to the gravity field were neglected (*9*) and if h'' were known over the entire planet, then the un-

known coefficients in the expression for gravitational potential energy, U, could be obtained from inversion of

$$U[\rho + h''(\theta,\phi),\theta,\phi] = -\frac{GM_{\venus}}{\rho + h''} \times$$

$$\left(1 + \sum_{n=1}^{\infty}\sum_{m=0}^{n}\left(\frac{\rho}{\rho + h''}\right)^n P_n^m(\sin\theta) \times\right.$$

$$\left. [C_{nm}\cos m\phi + S_{nm}\sin m\phi]\right) = U_0 \quad (8)$$

where G is the gravitational constant, $M_{\venus}$ the mass of Venus, $P_n^m(\sin\theta)$ the associated Legendre function of degree n and order m, C_{nm} and S_{nm} the sought-for coefficients, and U_0 the value of the potential on the reference contour. For data confined to the equatorial regions, as here, Eq. 8 can be recast as

$$\sum_{m=0}^{\infty}(C_m\cos m\phi + S_m\sin m\phi) \simeq \frac{h''(\phi)}{\rho} \quad (9)$$

where

$$\begin{bmatrix} C_m \\ S_m \end{bmatrix} \cong \sum_{n=m}^{\infty} P_n^m(0)\begin{bmatrix} C_{nm} \\ S_{nm} \end{bmatrix} \quad (10)$$

and where we set $U_0 \simeq -GM_{\venus}/\rho$ (10) and dropped terms of second order and higher in h''. The coefficients C_m and S_m are given by

$$\begin{bmatrix} C_m \\ S_m \end{bmatrix} = \frac{1}{\pi\rho}\int_0^{2\pi} h''(\phi)\begin{bmatrix} \cos m\phi \\ \sin m\phi \end{bmatrix} d\phi;$$

$$m = 1,2,\ldots \quad (11)$$

with $C_0 \simeq C_{00} = 1$ and $S_0 \equiv 0$. No useful information on the coefficients of the zonal harmonics (C_{n0}; $n \geq 2$) is contained in the equatorial portion of the equipotential contour, since the zonals have no longitude dependence and their bulk equatorial effect is not easily separable from that of $M_{\venus}$.

How may we use these results to estimate the gravitational torque exerted on Venus by the earth? For study of the putative spin-orbit resonance (2), the relevant torque is proportional to $(B - A)/C$ where $A < B < C$ are the principal moments of inertia of Venus, with C assumed to be the moment about the spin axis. Unless either (i) Venus is now a very elastic body (high "Q") with respect to the diurnal stresses of 100-day periodicity, or (ii) there exists a very delicate balance between the torques exerted by the sun on Venus' tidal bulge and on a possible atmospheric bulge (11), it appears that control of Venus' spin by the earth requires $(B - A)/C > 10^{-4}$ (2). If the tesseral

harmonics for Venus fall off with degree as do those for the moon and Mars, then the approximation

$$[(C_2)^2 + (S_2)^2]^{1/2} \simeq$$

$$3[(C_{22})^2 + (S_{22})^2]^{1/2} = 0.3\frac{B-A}{C} \quad (12)$$

should yield a reasonable estimate for $(B - A)/C$.

Unfortunately, data necessary to determine an accurate equipotential contour in the equatorial region of Venus do not now exist. The lack of both accurate values for $\kappa(h,\lambda)$ and properly calibrated radar cross-section data are the major limitations; in particular, there have been no coordinated observations of cross section at more than one radar frequency. If the variations with longitude of the intrinsic surface reflectivity are small and if the effects of the differences between total radar cross sections and cross sections per unit surface area at the subradar point are also small, we may use the limited data from the Haystack Observatory on the total cross sections (8) at $\lambda = 3.8$ cm, coupled with the surface-height variations recently determined (4), to obtain an approximate equipotential contour. The result is presented in Fig. 1 for $\kappa = 0.07$ km^{-1}. This choice for κ is based on Eq. 3 and the "nominal" values $P(0) = 100$ atm and $T(0) = 750°$K (12). A comparison with the surface-height variation (see Fig. 1) seems to indicate that minima in the equipotential contour are associated with topographic minima. But one must remember that the uncertainties are large; it is even difficult to place reliable bounds on the accuracy of the equipotential contour, in view of the lack of accurate and suitable data.

We can assess analytically the relative sensitivity of h'' to the various relevant factors. From Eqs. 1 through 7 we find, under conditions validating the last part of Eq. 5,

$$\delta h'' = \delta h' + \frac{1}{2\kappa(0,\lambda)}\frac{\delta\sigma}{\sigma} - h\frac{\delta\kappa(0,\lambda)}{\kappa(0,\lambda)} \quad (13)$$

The last term, through Eq. 3, can be separated into components due to errors in $T(0)$, $P(0)$, and numerical factors. On the basis of experimental and theoretical evidence relating to these components, we estimate that $|\delta\kappa/\kappa| < 0.6$. This contribution to h'' is proportional to h and may therefore be as much as several kilometers. For our nominal value of $\kappa(0,\lambda = 3.8$ cm$) \simeq 0.07$ km^{-1}, fractional errors in cross section of 10 percent will contribute errors of under 1 km to h''. The contribution of

$\delta h'$ (4) should be nowhere greater than about 0.5 km.

Unless the intrinsic surface reflectivity is well correlated with the surface altitude—unfortunately a not unlikely possibility—the solutions for C_2 and S_2, and hence the estimate for $(B - A)/C$, may be relatively immune to the effects of variations in intrinsic reflectivity. Under this assumption, we find from Fig. 1 and Eqs. 11 through 13 that

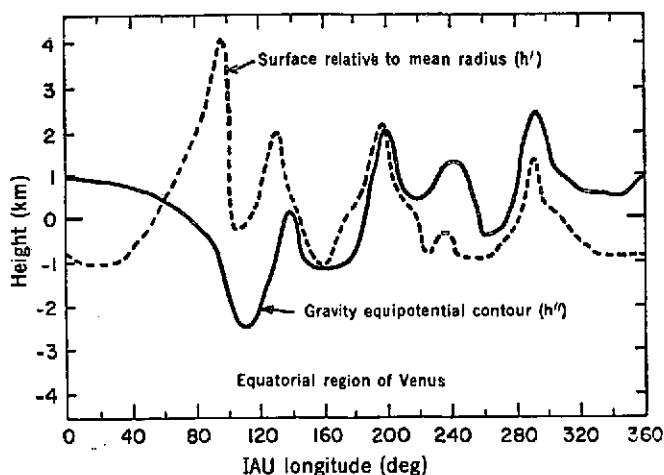$$\frac{B - A}{C} \simeq (3 \pm 3) \times 10^{-4} \quad (14)$$

where the error reflects our estimates of the uncertainties in κ, $c(\phi)$, and $h'(\phi)$. No allowance was made for the contributions of the higher-degree terms to C_2 and S_2 (13). We also find that the axis of minimum moment of inertia passes through longitude 30 ± 60 degrees [International Astronomical Union (IAU) coordinate system], which is too uncertain to allow meaningful deductions about torque balance.

The prospects for improvement in this very crude estimate of the gravity equipotential are good. Results from Venera 8, for example, should tighten the bounds on atmospheric composition, $T(0)$, and $P(0)$, and hence on κ (after laboratory confirmation or correction of Eq. 3). The radar systems at Arecibo, Puerto Rico ($\lambda = 70$ cm), Goldstone, California ($\lambda = 12.5$ cm), and at Haystack ($\lambda = 3.8$ cm) could be used to reduce the uncertainties in surface-height variations to the 150-m level or slightly below. With careful calibration of the radars, cross section measurements—for the same surface regions to which the height measurements apply—should have relative errors of no more than about 2 percent (8). Haystack's contribution is essential here, because there is no appreciable atmospheric absorption at the wavelengths used at the other observatories. Thus, earth-based measurements could yield gravity equipotential contours in the equatorial regions of Venus with a lateral surface resolution of about 100 km, corresponding to information on spherical harmonics up to the 360th degree, and an altitude resolution of about 200 m. The decrease in the uncertainty of the estimate of $(B - A)/C$ should be at least fourfold if the higher harmonics do not contribute too much to C_2 and S_2.

Can the determination of Venus' gravity equipotential contour be extended beyond the equatorial regions traversed by the subearth point? Two approaches are possible. (i) With more

Fig. 1. Comparison of the surface heights on Venus with a gravity equipotential contour. The surface heights are based on round-trip radar echo delays from published (4) and recent, unpublished data. The gravity potential contour is derived from data on radar cross sections obtained at the Haystack Observatory (8); the uncertainties in both the scale and variations of

this latter curve are large (see text). Latitude variations have been suppressed, with both curves referring to averages along a narrow (± 10°) band centered on the equator of Venus.

powerful earth-based radar systems, such as the proposed improved Arecibo facility, it will be possible to determine surface heights and reflectivities over most of the planet with high resolution by use of the new technique of delay-Doppler interferometry (14) at the 12.5-cm wavelength at which this radar would operate. If a similar capability existed for shorter radar wavelengths, such as with a Haystack-Goldstone bistatic configuration, then the atmospheric absorption could be determined as well. Of course, in the analysis of these data—for which the incident and reflected waves would not be in the zenith direction on Venus—atmospheric refraction effects must be considered (7) as well as possible variations of the intrinsic angular scattering law with frequency (3). (ii) A spacecraft placed in a polar, or near-polar, orbit about Venus and equipped with a suitable dual-frequency radar, could determine surface heights, reflectivities, and the corresponding atmospheric absorptions over virtually the entire planet. Repeated polar passages would offer the possibility for continual calibration. The resultant high-resolution equipotential

contours would not only yield the gravitational torque exerted by the earth but would have other scientific applications as well: these contours bear, for example, on questions of the origin and evolution of Venus, its deep interior, the extent of isostatic compensation near its surface, and the processes of surface erosion (15).

IRWIN I. SHAPIRO
GORDON H. PETTENGILL
GARY N. SHERMAN
Department of Earth and Planetary Sciences, Massachusetts Institute of Technology, Cambridge 02139
ALAN E. E. ROGERS
RICHARD P. INGALLS
Haystack Observatory,
Westford, Massachusetts 01886

References and Notes

1. R. M. Goldstein, in Moon and Planets, A Dollfus, Ed. (North-Holland, Amsterdam, 1967), p. 126; I. I. Shapiro, Science 157, 423 (1967); R. F. Jurgens, Radio Sci. 5, 435 (1970); R. L. Carpenter, Astron. J. 75, 61 (1970).
2. P. Goldreich and S. J. Peale, Astron. J. 72, 662 (1967); E. Bellomo, G. Colombo, I. I. Shapiro, in Mantles of the Earth and Terrestrial Planets, S. Runcorn, Ed. (Interscience, New York, 1967), p. 219.
3. Radar observations of the moon, Mercury, and Mars show rather slight variations in cross section with frequency [see, for ex-

ample, J. V. Evans and T. Hagfors, Eds., Radar Astronomy (McGraw-Hill, New York, 1968)]. Possible significant absorption by clouds is probably not of prime importance for two related reasons. (i) If the clouds are uniformly distributed over the planet with either a known or a weak microwave frequency dependence, there will be no problem (in fact the Mariner Venus-Mercury flyby mission in 1974 will allow this absorption to be measured at both S-band and X-band). (ii) If the clouds are nonuniformly distributed, their contribution will probably vary with time, thereby allowing the variable parts to be estimated.
4. D. B. Campbell, R. B. Dyce, R. P. Ingalls, G. H. Pettengill, I. I. Shapiro, Science 175, 514 (1972).
5. The apparent lack of substantial temperature variations over the surface of Venus (A. C. E. Sinclair, J. P. Basart, D. Buhl, W. A. Gale, Astrophys. J., in press) supports the assumption that pressure contours coincide with gravity equipotential contours. Meteorological distortions of this identification, unless static, would be discernible from repeated observations at different solar orientations.
6. W. Ho and I. A. Kaufman, J. Chem. Phys. 45, 877 (1966); W. Ho, I. A. Kaufman, P. Thaddeus, J. Geophys. Res. 71, 5091 (1966).
7. M. A. Slade and I. I. Shapiro, J. Geophys. Res. 75, 3301 (1970).
8. A. E. E. Rogers, R. P. Ingalls, L. P. Rainville, Astron. J. 77, 100 (1972); W. B. Smith, R. P. Ingalls, I. I. Shapiro, M. E. Ash, Radio Sci. 5, 411 (1970).
9. The centrifugal acceleration can be neglected because of both the slow rotation of Venus and the constancy of the contribution in the equatorial regions.
10. Strictly speaking, we should take $U_0 = U(R,0,\phi_0)$; however, our approximation is consistent with the neglect of higher-order terms in h''.
11. T. Gold and S. Soter, Icarus 14, 16 (1971).
12. These values are closer to the Venera findings than those used in (8); the reference longitude (see text) was chosen such that the values apply to the mean radius of 6050 km (4).
13. The analysis of the Mariner 5 radio tracking data [J. D. Anderson and L. Efron, Bull. Amer. Astron. Soc. 1, 231 (1969)] yielded an upper bound on $[C - (A + B)/2]/M_0\rho^2$ of 10^{-5}, which is difficult to reconcile with a value of $(B - A)/C$ of the order of 10^{-4}. Aside from (remote) possibilities, such as Venus not spinning about its axis of maximum moment of inertia, the discrepancy may be explained by errors in the values used for κ and $\sigma(\phi)$ or by an unrealistic bound for the tracking data, or by a combination.
14. I. I. Shapiro, S. H. Zisk, A. E. E. Rogers, M. A. Slade, T. W. Thompson, Science 178, 939 (1972).
15. The earth-spacecraft radio tracking data will also be sensitive to variations in the gravity potential, but only to the harmonics of relatively low degree and order. For these, the tracking data can serve to check the results from the direct observations of the surface at two frequencies, and perhaps to calibrate $\kappa(0,\lambda)$.
16. Research at the Haystack Observatory is supported by NSF grant GP-25865 and NASA grant NGR 22-174-003, contract NAS 9-7830.

12 October 1972